Supporting Information

Rational design of Au nanorods assemblies for highly sensitive and selective SERS detection of prostate specific antigen

An-qi Yang, [a] Dong Wang, [a,b] Xiang Wang, [b] Yu Han,[a] Xue-bin Ke, [a] Hong-jun Wang, [c] Xi Zhou* [a] and Lei Ren* [a,b]

[a] Department of Biomaterials, College of Materials, Xiamen University, Xiamen, 361005, People's Republic of China.

[b] State Key Laboratory for Physical Chemistry of Solid Surfaces, Department of Chemistry, College of Chemistry and Chemical Engineering, Xiamen University, Xiamen, 361005, People's Republic of China.

[c] Department of Chemistry, Chemical Biology and Biomedical Engineering, Stevens Institute of Technology, 1 Castle Point on Hudson, Hoboken, New Jersey, 07030, USA.

Correspondence should be addressed to Dr. Xi Zhou, Email: xizhou@xmu.edu.cn; Tel: +86-592-2188530; Fax: +86-592-2183937.

1. TEM and absorption spectra characterization of AuNRs

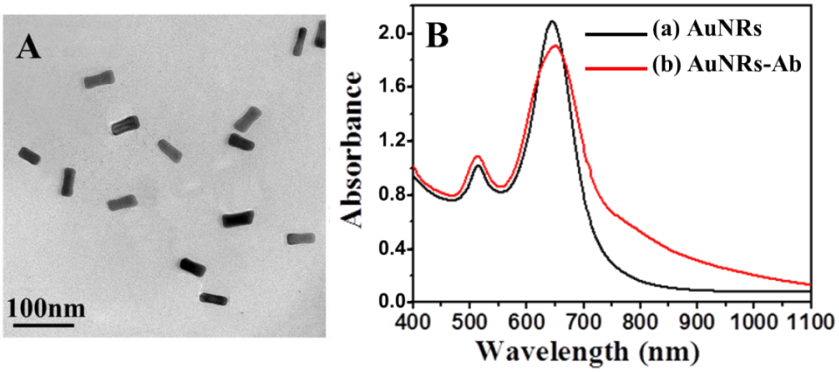

Fig. S1 (A) TEM image of Au NRs; (B) UV-vis spectroscopy of (a) AuNRs and (b) AuNR-Ab.

2. Surface zeta potential and FTIR characterization of AuNRs functionalized with antibody

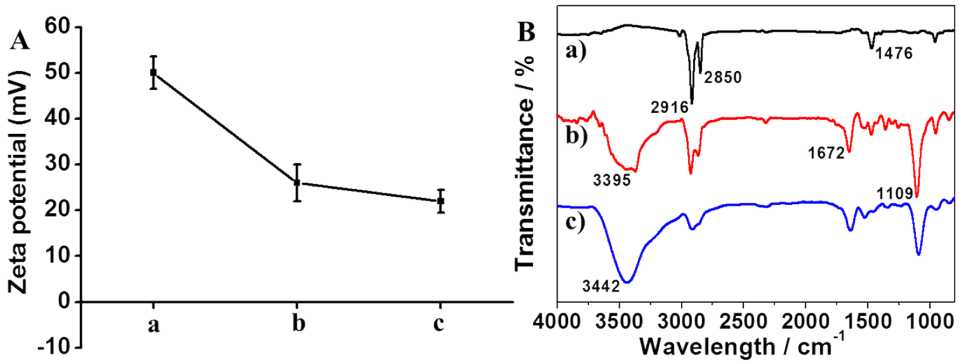

Fig. S2 (A) The zeta potential and (B) FT-IR spectra of AuNRs in various stages: (a) initial AuNRs sample, (b) HS-PEG-COOH modified AuNRs sample, (c) antibody functionalized AuNRs samples.

The evolution of preparation and functionalization of AuNRs was further evaluated by FTIR spectra (Fig. S1B). AuNRs (Fig. S2B(a)) revealed strong peaks at 2916 and 2850 cm^{-1} (C–H stretch) due to the existence of large amount of CTAB.[1] Also a characteristic peak existed at 1476 cm^{-1} (C–H asymmetrical stretch), which was from the CH_3–N^+ moiety of CTAB.[2] In the spectrum of Fig. S2B(b), C-O stretching at 1109 cm^{-1}, C=O stretching at 1672 cm^{-1} and O-H stretching at 3395 cm^{-1} indicated the successful functionalization of HS-PEG-COOH.[3] After the further addition of antibody into AuNRs, a broad band of the N-H or -NH_2 groups at 3442 cm^{-1} was strengthened,[4] which might verify the attachment of antibody on the surface of AuNRs (Fig. S2B(c)).

3. Quantitative analysis of antibodies conjugated to per AuNR

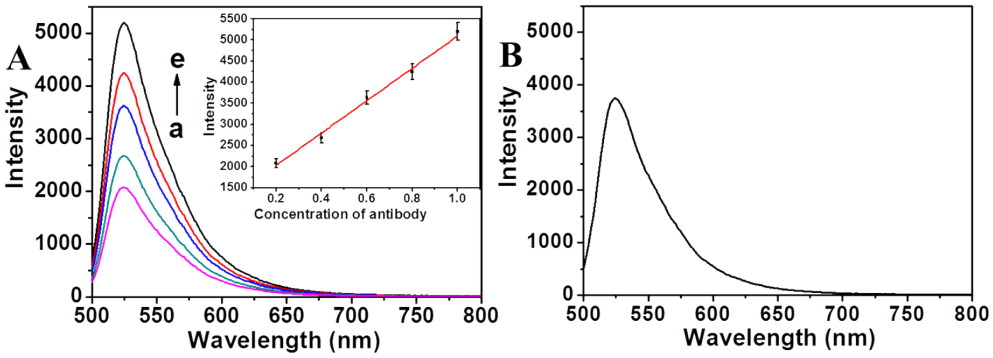

Fig. S3 (A) Fluorescence spectra of antibody-FITC with different concentration (a-e: 0.2, 0.4, 0.6, 0.8, 1.0 μg/mL). Inset: The calibration curve between fluorescence intensity (525 nm) and antibody-FITC concentration. (B) Fluorescence spectra of the supernatant separated from antibody-FITC and AuNRs reaction solution (the un-conjugated antibody-FITC). The excitation and emission wavelengths were 488 nm and 525 nm, respectively.

Fluorescence quantitative assay was used to determine the number of antibodies conjugated to per AuNR (Fig. S3). Upon increasing the concentration of antibody-FITC, the fluorescence intensity increased. The linear relationship of antibody-FITC concentration and fluorescence signal intensity at 525 nm peak was presented in inset figure. The regression equation was Y=3829.29X+1263.92, with a good correlation coefficient (R^2 = 0.991), where X was the concentration of antibody-FITC and Y was the fluorescence intensity of the sample detected. The calibration curve can be used to determine the concentration of antibody conjugated to AuNRs, indirectly. As mentioned in the experimentation section, the detector antibody-FITC (15 μL, 50 μg/mL) was added to the mixture (500 μL) and stirred for 3 min at room temperature. After incubating at 37 °C for 1 h, the mixture was purified by centrifugation for 15 min at 6,500 rpm. The un-conjugated antibody-FITC present in the supernatant was analyzed via fluorescence spectrophotometer, the result has been shown in Fig. S3B. By applying the regression equation, the concentration of antibody in supernatant was 0.65 μg/mL (19.13 nM), and the concentration of antibody conjugated to AuNRs was calculated to be 0.85 μg/mL (25.02 nM).

Here the particle concentration of AuNRs was determined through absorbance, and calculated by Lambert-Beer law:[5] C=A/(αb), where A was absorbance of longitudinal plasmon peak (measured to be 2.12 in Fig S1B), α was absorption coefficient ($3.9\pm0.5\times10^9$ $M^{-1}\cdot cm^{-1}$),[6] b was the length of the light path (1 cm), hence concentration of AuNRs was calculated to be 0.544 nM.

Therefore, the amount of antibody conjugated to AuNRs was calculated to be 25.02/0.544=46. As mentioned in Scheme.1 of main text, almost all of the antibodies were anchored to the end face of AuNRs, which means there were 46 antibodies packed on each rip of AuNR assembly.

Based on the current characterization, it is hard to accurately determine how many PSA molecules are linked between the two AuNRs. We try to calculate it according to the fluorescence and absorption quantitative assay, as well as the TEM observation. As displayed in Fig. 4B, the immunosensor exhibited the strongest SERS enhancement with the addition of 100 ng/mL PSA (3.3 nM), which means the AuNRs reach the longest end-to-end assembly at this concentration

point. The assembly rate at this status was about 58%, as being recorded via TEM observation. Thus, the number of PSA molecules linked between the two AuNRs was estimated to be 3.3/(0.544*0.58)=10. However, we reasonably assume that some of the PSA molecules may be linked to the unassembled AuNR. At this situation, the number of PSA molecules linked between the two AuNRs was estimated to be 3.3/0.544=6. Therefore, the number of PSA molecules linked between the two AuNRs ranged from 6 to 10.

4. **SERS-based Human Alpha Fetoprotein (AFP) immunoassay**

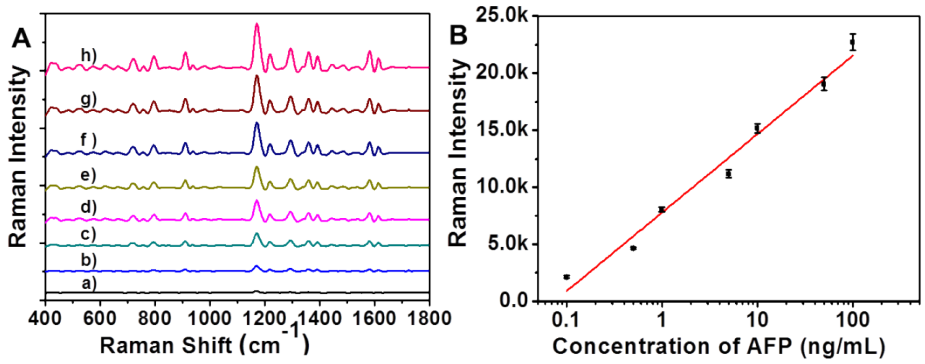

Fig. S4 (A) SERS spectra of MGITC-labeled AuNRs assembly incubated with different concentrations of AFP: (a) - (h) 0, 0.1, 0.5, 1, 5, 10, 50, 100 ng/mL. (B) The calibration curve between Raman intensity (1172 cm^{-1} peak) and AFP concentration.

5. Characterization of AuNRs assembly directed by antibody-AFP biorecognition

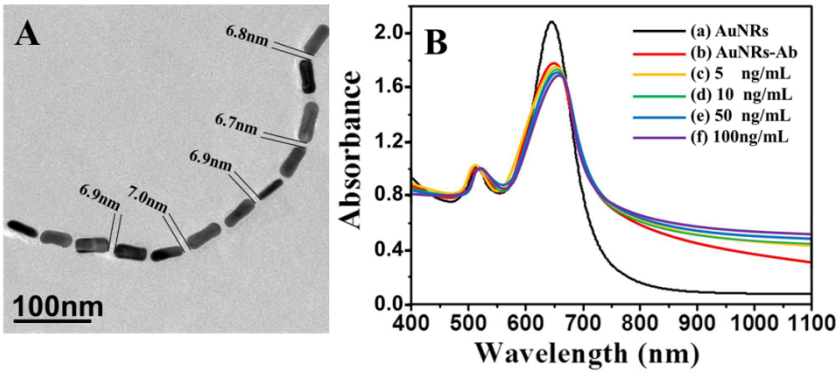

Fig. S5 (A) Representative TEM images of AuNRs EE assembly formed with the addition of AFP. (B) UV-vis spectroscopy of (a) AuNR, (b) AuNR-Ab and (c) - (f) AuNRs-Ab solution incubated with different concentrations of AFP: 5, 10, 50, 100 ng/mL.

Compared with PSA detection, the linear range of the AFP concentration was relatively narrower. To explain this issue, further investigation of the AuNRs assembly directed by AFP was conducted *via* TEM and UV–vis spectroscopy. As shown in Fig. S5A, the distance between consecutive AuNRs was 6.90±0.25 nm, which was larger than that of PSA directed AuNRs assembly. The variation in the optical properties of AuNRs assembly was demonstrated by UV–vis spectroscopy (Fig. S5B). As the concentration of AFP gradually increasing, the red-shift of the longitudinal plasmon peak was relatively smaller (from 648 to 653 nm) than that of PSA directed

AuNRs assembly.

According to the study of El-Sayed[7] and Mulvaney et al.,[8] the plasmon coupling (PC) between the assembled AuNRs was highly distance-dependent, the intensity of PC was found to decrease with increasing distance between AuNRs. Moreover, the electric-field enhancement decreases with the increasing of the interparticle spacing.[9] AFP and PSA are macromolecules, the molecular weight of AFP (69 KDa)[10] is higher than that of PSA (30 KDa),[11] which indicates AFP may have a larger spatial size than PSA. Thus, the distance between AFP directed AuNRs assembly was larger than that induced by PSA. As a consequence, the PC and electric-field in the gap between AFP directed AuNRs assembly might be relatively weaker, resulting in the smaller red-shift of the longitudinal plasmon peak and weaker SERS enhancement than that of PSA directed AuNRs assembly.

References

1. H. Tang, S. Shen, J. Guo, B. Chang, X. Jiang and W. Yang, *J. Mater. Chem.*, 2012, **22**, 16095.
2. B. Nikoobakht and M. A. El-Sayed, *Langmuir*, 2001, **17**, 6368.
3. P. Harder, M. Grunze, R. Dahint, G. M. Whitesides and P. E. Laibinis, *J. Phys. Chem.*, 1998, **102**, 426.
4. B. D. Chithrani, A. A. Ghazan and C. W. Chan, *Nano Lett.*, 2006, **6**, 662.
5. S. Liang, M. Yi, Z. Shen, L. Liu, X. Zhang and S. Ma, *RSC Adv.*, 2014, **4**, 16127
6. C. J. Orendorff and C. J. Murphy, *J. Phys. Chem. B*, 2006, **110**, 3990.
7. P. K. Jain, S. Eustis and M. A. El-Sayed, *J. Phys. Chem. B*, 2006, **110**, 18243.
8. A. M. Funston, C. Novo, T. J. Davis and P. Mulvaney, *Nano letters*, 2009, **9**, 1651.
9. L. Q. Lin, E. Crew, H. Yan, S. Shan, Z. Skeete, D. Mott, T. Krentsel, J. Yin, N. A. Chernova, J. Luo, M. H. Engelhard, C. Wang, Q. B. Li and C. J. Zhong, *J. Mater. Chem. B*, 2013, **1**, 4320.
10. L. Chuang, J. Y. Hwang, H. C. Chang, F. M. Chang and S. B. Jong, *Clin. Chim. Acta*, 2004, **348**, 87.
11. E. A. Stura, B. H. Muller, M. Bossus, S Michel, C. Jolivet-Reynaud and F. Ducancel, *J. Mol. Biol.* 2011, **414**, 530.